Title
Soil carbon sensitivity to temperature and carbon use efficiency compared across microbial-ecosystem models of varying complexity

Journal
Biogeochemistry, 119(1-3)

ISSN
0168-2563

Authors
Li, Jianwei
Wang, Gangsheng
Allison, Steven D
et al.

Publication Date
2014-06-01

DOI
10.1007/s10533-013-9948-8

Peer reviewed

Soil carbon sensitivity to temperature and carbon use efficiency compared across microbial-ecosystem models of varying complexity

Jianwei Li[1], Gangsheng Wang[2], Steven D. Allison[3,4], Melanie A. Mayes[2], Yiqi Luo[1]

1. Department of Botany and Microbiology, University of Oklahoma, Norman, OK 73019
2. Climate Change Science Institute and Environmental Sciences Division, Oak Ridge National Laboratory, Oak Ridge, TN 37831-6301
3. Department of Ecology and Evolutionary Biology, University of California, Irvine, California 92697
4. Department of Earth System Science, University of California, Irvine, California 92697

Abstract. Global ecosystem models may require microbial components to accurately predict feedbacks between climate warming and soil decomposition, but it is unclear what parameters and levels of complexity are ideal for scaling up to the globe. Here we conducted a model comparison using a conventional model with first-order decay and three microbial models of increasing complexity that simulate short- to long-term soil carbon dynamics. We focused on soil carbon responses to microbial carbon use efficiency (CUE) and temperature. Three scenarios were implemented in all models at a common reference temperature (20°C): constant CUE (held at 0.31), varied CUE (-0.016°C^{-1}), and 50% acclimated CUE (-0.008°C^{-1}). Whereas the conventional model always showed soil carbon losses with increasing temperature, the microbial models each predicted a temperature threshold above which warming led to soil carbon gain. The location of this threshold depended on CUE scenario, with higher temperature thresholds under the acclimated and constant scenarios. This result suggests that the temperature sensitivity of CUE and the structure of the soil carbon model together regulate the long-term soil carbon response to warming. Equilibrium soil carbon stocks predicted by the microbial models were much less sensitive to changing inputs compared to the conventional model. Although many soil carbon dynamics were similar across microbial models, the most complex model showed less pronounced oscillations. Thus adding model complexity (i.e. including enzyme pools) could improve the mechanistic representation of soil carbon dynamics during the transient phase in certain ecosystems. This study suggests that model structure and CUE parameterization should be carefully evaluated when scaling up microbial models to ecosystems and the globe.

Key words: Warming, soil organic matter decomposition, first-order decay model, microbial-enzyme model, carbon use efficiency, temperature threshold, microbial acclimation, model complexity

1. Introduction

Soil carbon (C) is the largest organic C pool in terrestrial biosphere (Jobbagy and Jackson 2000). Microbial communities are the primary drivers of soil organic matter (SOM) decomposition, and climate change effects on microbial physiology can affect the rates of C cycling processes (Bradford et al. 2008, Malcolm et al. 2008). Therefore, accounting for the response of microbial communities to environmental parameters in Earth system models may be needed to adequately predict feedbacks between global change and the decomposition of soil organic C (Friedlingstein et al. 2006, Thornton et al. 2009). Recently, model simulations of global soil C stocks were substantially improved by integrating microbial processes (Wieder et al. 2013). Such microbial models hold promise for improving predictions of climate effects on soil decomposition, yet the regulatory mechanisms governing microbial processes remain a major gap in understanding (Ågren and Wetterstedt 2007).

Extracellular enzymes produced by microbes are responsible for the degradation of complex organic C that is ultimately taken up by microbial biomass and released to the atmosphere as CO_2 (Sinsabaugh et al. 1991, Schimel and Weintraub 2003). In contrast to the assumptions of conventional first-order decomposition models (Parton et al. 1988), SOM decomposition rates depend on not only the size of the soil C pool but also on the size and composition of the decomposer microbe pool (Schimel and Weintraub 2003). As climate changes, soil carbon stocks will likely depend on sequestration and loss pathways regulated by microbial physiology (Schimel 2013), and first-order models may have difficulty simulating climate responses over short time scales (Manzoni and Porporato 2007, Lawrence et al. 2009). Yet even with recent advances in microbial models, nearly 50% of the spatial variation in global

67 soil C stocks is still unexplained (Wieder et al. 2013). Therefore, identifying accurate and simple
68 models at microbial to ecosystem scales is essential for improving global soil models.
69 Microbial growth depends on carbon use efficiency (CUE), defined as the fraction of C
70 uptake allocated to growth (del Giorgio and Cole 1998). In general, CUE decreases as
71 temperature increases, but terrestrial decomposers show variable CUE responses to temperature
72 (Manzoni et al. 2012). CUE also varies with decomposer group and substrate chemistry (Six et
73 al. 2006, Frey et al. 2013). This variation implies that CUE responses may change across
74 environmental gradients. For example, CUE acclimation under warming can explain declines in
75 soil respiration, microbial biomass, and enzyme activity following an ephemeral increase in soil
76 respiration (Allison et al. 2010, Zhou et al. 2012). In the longer term, adaptive mechanisms that
77 make a microbial community more efficient at decaying stable SOM could enhance the positive
78 feedback between soil and climate (Frey et al. 2013). However, conventional models that
79 assume first-order decay during SOM decomposition do not include these mechanisms (Todd-
80 Brown et al. 2012). As a key variable in microbial function, parameterizing CUE and its
81 response to temperature is essential for predicting soil responses to climate change (Luo et al.
82 2001, Bradford et al. 2008).
83 Recently, several microbial models have been developed to simulate warming effects on
84 SOM decomposition (Allison et al. 2010, German et al. 2012, Wang et al. 2013a). These models
85 are similar in basic structure and key biogeochemical processes but differ in model complexity
86 and reference temperature. Although such models are now being used at the global scale
87 (Wieder et al. 2013), there have been few efforts to compare model structures and behaviors
88 relevant to this scaling process. Specifically, we asked how microbial model predictions change
89 with increasing model complexity, and whether these predictions differ fundamentally from

models with a conventional structure. As much as possible, we standardized parameters across four focal models and compared their predictions for soil C in response to temperature variation under three CUE scenarios. We hypothesized that model predictions would vary widely based on CUE and its temperature response. We also expected that the magnitude of soil C response would be damped in models with more C pools. This type of model comparison can help identify the fundamental microbial mechanisms regulating soil responses to warming and the appropriate level of mathematical complexity for future microbial models (Todd-Brown et al. 2012).

2. Model structures

We compared microbial models from German et al. (2012), Allison et al. (2010), and Wang et al. (2013), referred to here as GER, AWB, and MEND, respectively. We also analyzed the conventional model described in Allison et al. (2010) and referred to here as CON (Fig. 1). The CON model includes two soil C pools and a microbial C pool that produce CO_2 through first-order decay, similar to structures used in current Earth system models (Todd-Brown et al. 2012). The differential equations underlying all four models are given in Appendix A.

The microbial models share a similar structure characterized by dependence of soil C fluxes on microbial biomass pools (Fig. 1). GER is the simplest microbial model with a single soil organic C (SOC) pool whose decomposition rate depends on microbial biomass C (MBC). AWB has two additional pools: extracellular enzyme C (ENZC) and dissolved organic C (DOC). DOC is produced from SOC as a function of ENZC, and MBC takes up DOC and produces ENZC. MEND is the most complex model with SOC divided into particulate (POC) and mineral organic C (MOC), and ENZC divided into particulate (EP) and mineral enzymes (EM). MEND

also includes a mineral-adsorbed phase of DOC (i.e., QOC) regulated by temperature-dependent (Arrhenius) adsorption-desorption kinetics.

In all microbial models, C inputs enter the SOC and/or DOC pools at a constant rate. SOC decomposition and DOC uptake follow the Michaelis-Menten equation (Eq. 1), and the maximum reaction rate and half saturation constant follow Arrhenius temperature dependence, which we express here in the form of Eq. 2,

$$Y(T) = \frac{V(T) \times EB \times C}{K(T) + C} \tag{1}$$

$$V(T) = V(T_{\text{ref}}) \cdot \exp\left[-\frac{Ea}{R}\left(\frac{1}{T} - \frac{1}{T_{\text{ref}}} \right) \right] \tag{2}$$

where $Y(T)$ is the C flux for SOC decomposition or DOC uptake; $V(T)$, EB, C, and $K(T)$ denote the maximum reaction rate, enzyme or microbial biomass, substrate concentration, and half saturation constant, respectively; $V(T_{ref})$, Ea, R, and T denote the maximum reaction rate at reference temperature (T_{ref}), energy of activation (kJ mol^{-1}), gas constant (8.314 J mol^{-1} K^{-1}) and simulation temperature (Kelvin), respectively. The half saturation constants also follow an Arrhenius relationship with temperature (Eq. 2). The original version of AWB used a linear relationship, but we used the Arrhenius relationship here to make the models more comparable.

In all three microbial models, C is lost through growth respiration dependent on CUE following uptake of organic C. MEND also includes a separate term for maintenance respiration with Arrhenius temperature dependence (Wang and Post 2012). All models assume that carbon use efficiency (CUE, E_C) varies with temperature based on a linear relationship (Devevre and Horwath 2000):

$$E_C(T) = E_{C,ref} + m \times (T - T_{ref}) \quad (3)$$

where $E_C(T)$, $E_{C,ref}$, and m denote the CUE at simulation temperature T, the reference temperature (T_{ref}), and the temperature response coefficient (°C $^{-1}$), respectively.

Aside from their structure, the models in our analysis also differ in parameters (Table A1). If the same parameter was included in multiple models, we used the parameter values from Wang et al. (2013) to make model predictions more comparable. For unique parameters, we generally used parameter values given with the published version of the model. Because we hypothesized that the models would be particularly sensitive to changes in CUE, we ran the models under three CUE scenarios. In the "constant CUE" scenario, $m = 0$, such that CUE was constant at 0.31 under different temperatures. This CUE is close to the value of 0.30 recently suggested for terrestrial ecosystems (Sinsabaugh et al. 2013). In the "varied CUE" scenario, m = –0.016ºC^{-1}, as in Allison et al. (2010). Finally, the "acclimated CUE" scenario mimics 50% thermal acclimation of microbial physiology with m = –0.008ºC^{-1}. All scenarios used T_{ref} = 20°C and $E_{C,ref}$ = 0.31. CON does not include an explicit CUE, but the coefficients that specify partitioning of fluxes into CO_2 versus C pools are analogous. Therefore we applied the CUE scenarios to CON by setting these partition coefficients equal to the CUE values from each scenario.

To test model sensitivities to temperature and CUE scenario, we analyzed C pools and CO_2 efflux at equilibrium and during the transient phase following temperature increase. Equilibrium pool sizes and efflux were determined analytically by solving the differential equations for each model at steady state (Appendix A). Transient dynamics were simulated following perturbation of the equilibrium model state at 20°C under constant, varied and

acclimated CUE scenarios. Simulations were run for 100 years at 25°C, representing 5°C warming. By definition, CO_2 efflux must always return to the equilibrium value (equal to inputs) because respiration is the only output flux in these models. We report relative changes (%) in C pool sizes and CO_2 efflux compared to equilibrium values at the reference temperature under different CUE scenarios and between models.

Because we are ultimately interested in how model predictions will differ under climate change, we conducted a detailed temperature sensitivity analysis. Warming can induce two opposite effects on SOC decomposition in microbial models. First, temperature increase enhances maximum reaction rates for SOC decomposition and DOC uptake by microbes (Eqs. 1 and 2). Second, warming decreases CUE which then reduces microbial biomass and enzyme production. Because MBC or ENZC is a controlling variable in Eq. 1, the decrease in CUE due to warming could act as negative feedback on SOC decomposition and DOC uptake. That is, there must exist a threshold temperature at which the decline in microbial biomass exactly offsets the positive effect of warming on C decomposition and uptake. We determined this threshold temperature in both models at steady state across a range of *m* values.

3. Results

3.1 Soil decomposition dynamics at steady state

Under the reference temperature (i.e. 20°C) and parameterization, steady state C pool sizes differed somewhat between models (Table 1). CON and AWB had similar SOC (33.3 vs. 37.8 mg C g^{-1} soil) with more SOC in MEND and less in GER. MBC was similar in all three microbial models (0.25-0.26 mg C g^{-1} soil), but substantially lower in CON. DOC was similar in AWB and CON (0.03-0.04 mg C g^{-1} soil) but nearly five-fold greater in MEND. ENZC was

only 0.0014 mg C g^{-1} soil and almost identical in AWB and MEND. MOC and POC pools in MEND were about 85% and 13% of SOC, respectively, with the remaining pools accounting for < 2% of SOC; QOC was 5.4 times DOC at steady-state.

The CON model showed consistent declines in SOC, DOC, and MBC pools with increasing temperature across all CUE scenarios, which contrasts with the range of responses predicted by the microbial models (Fig. 2). Most steady-state pools in the microbial models changed with temperature, with the direction of change depending on the CUE scenario and model (Fig. 2). However, DOC and QOC temperature responses in MEND were similar across all CUE scenarios (Fig. S1). Subsequently, we present the changes in each specific C pool with temperature under each CUE scenario and across the four models. The results below are presented in Fig. 2 and Fig. S1 unless otherwise noted.

SOC: Under constant CUE, SOC declined with increasing temperature in all models but with greater relative changes in AWB and MEND than in CON and GER at lower temperatures (Fig. 2). Under varied and acclimated CUE scenarios, SOC response to temperature differed between CON and the microbial models (Fig. 2). In CON, SOC always monotonically decreased with increasing temperature. In the microbial models, equilibrium SOC declined with increasing temperature to a point but then increased again. This point, or temperature threshold, was higher in GER than in the other microbial models and increased with greater acclimation of CUE (Fig. 3). Under varied CUE, minimum SOC in AWB and MEND occurred at 1.45°C and 0.90°C, corresponding to CUEs of 0.61 and 0.62, respectively. The temperature threshold for GER under the varied CUE scenario was 7.95°C (corresponding CUE = 0.50). Under acclimated CUE, SOC declined with temperature in AWB and MEND up until thresholds of 19.15°C and 18.65°C (CUE = 0.317 and 0.321, respectively), whereas the threshold in GER under this scenario was

198 21.80°C (CUE = 0.236). Thus as CUE became less sensitive to temperature (greater
199 acclimation), the temperature threshold for minimum equilibrium SOC shifted to warmer values
200 (Fig. 3). If there is no CUE temperature sensitivity (constant CUE scenario), the microbial
201 models converge on the CON prediction of monotonic decline in SOC storage with increasing
202 temperature (Fig. 3).
203 In MEND, equilibrium MOC responses were nearly identical to SOC in all CUE
204 scenarios (Fig. S1). In contrast, equilibrium POC increased at a slower rate than SOC and MOC
205 as temperature declined (Fig. S1).
206 *DOC:* In CON, equilibrium DOC monotonically decreased with increasing temperature
207 under all CUE scenarios (Fig. 2). In AWB, DOC followed SOC under each CUE scenario. In
208 contrast, DOC always increased with increasing temperature in MEND, and the magnitude of
209 increase was identical across CUE scenarios (Fig. 2). QOC always declined with increasing
210 temperature in MEND, and the decline was also identical across CUE scenarios (Fig. S1).
211 *ENZC:* The ENZC response to temperature was identical between AWB and MEND with
212 no change under constant CUE and greater declines with increasing temperature from acclimated
213 to varied CUE scenarios (Fig. 2). In MEND, EM and EP responses to temperature both tracked
214 ENZC in all CUE scenarios with the greatest declines with increasing temperature under the
215 varied CUE scenario (Fig. S1).
216 *MBC:* Equilibrium MBC generally declined with increasing temperature except in GER
217 and AWB under constant CUE where there was no change (Fig. 2). The MBC response to
218 temperature was identical to ENZC in AWB. The magnitude of MBC changes with temperature
219 depended on CUE scenario, with the greatest declines in the varied CUE scenario and the
220 smallest changes in the constant CUE scenario for the three microbial models. The magnitudes

221 of MBC change predicted by all models followed the order: CON > MEND > AWB = GER
222 below the reference temperature (i.e. 20°C).
223 *3.2 Soil decomposition dynamics during transient phase*
224 Most C pools and CO_2 efflux reached steady state after 50-100 years in all models, except
225 those in GER, which required 100 years or more to reach steady state (Fig. 4). Transient
226 responses to 5ºC warming differed between CON and the microbial models. With CON, all pool
227 sizes declined monotonically to equilibrium whereas the microbial models showed oscillations
228 during the transient phase. These oscillations had the greatest magnitude in GER and the highest
229 frequency in MEND. Oscillations tended to be weakest in the acclimated CUE scenario and
230 strongest in the varied CUE scenario, which also showed the largest absolute change in SOC at
231 equilibrium. The amplitude of the oscillations was largest for CO_2 efflux, with the range
232 exceeding 100% relative change for GER and AWB in the early years of the constant and varied
233 CUE scenarios. The dynamics for MBC and ENZC were similar to CO_2 but with slightly lower
234 magnitudes of oscillation. In MEND, MOC dynamics were similar to total SOC but with weaker
235 oscillations. Most of the oscillation in MEND SOC was driven by strong oscillations in POC,
236 especially during the first 40 years and in the varied CUE scenario (Fig. S2).
237 Equilibrium responses to a step increase of 5ºC from the numerical simulations were
238 consistent with analytical solutions as a function of temperature. Warming reduced equilibrium
239 SOC in all models under constant CUE but increased SOC in the microbial models under varied
240 and acclimated CUE scenarios (Fig. 4). Equilibrium DOC showed little response to warming in
241 MEND, but declined under constant CUE and increased under varied CUE in AWB. Across all
242 models, equilibrium MBC declined more with warming as the temperature sensitivity of CUE
243 increased. The magnitude of decline followed the order CON > MEND > AWB = GER

244 regardless of CUE scenario. In AWB and MEND, the warming response of equilibrium ENZC
245 was similar to MBC, although the equilibrium ENZC was identical in the two models, unlike
246 with MBC. EP and EM in MEND showed warming responses very similar to total ENZC (Fig.
247 S2). Equilibrium CO_2 efflux always converged on 0% relative change in all models and
248 scenarios, consistent with inputs = outputs at steady state (Fig. 4).
249
250 **4. Discussion**
251 *4.1 Model comparison*
252 Based on the model analytical solutions, CON showed fundamentally different responses
253 to temperature and CUE change relative to the microbial models (Fig. 3). The microbial models,
254 while differing in the number of pools and some parameter values, generally showed similar
255 responses to temperature and CUE change. For example, the steady-state SOC pool in CON was
256 proportional to SOC inputs and inversely proportional to the SOC decay constant, which
257 increased exponentially with temperature (Eq. A10). Thus the main effect of temperature
258 increase in CON was to increase the decay constant and reduce the equilibrium SOC pool. In
259 contrast, SOC in the microbial models depended primarily on microbial parameters. In GER for
260 example, equilibrium SOC was proportional to microbial turnover and enzyme K_m but inversely
261 proportional to CUE and enzyme V_{max} (Eq. A17). As temperature increases in the microbial
262 models, the direction of SOC change depends on the balance between increases in K_m and
263 declines in CUE, both of which tend to increase SOC, and increases in V_{max}, which tend to
264 reduce SOC.
265 *4.2 CUE and model complexity influence soil C response to warming*

We found that the microbial models, but not CON, predicted a threshold temperature corresponding to minimum soil C storage (Fig. 3). This threshold is important because it determines whether warming causes an increase or decrease in soil C storage in a given ecosystem. Cooler ecosystems with mean temperatures below the threshold should lose soil C with warming, whereas ecosystems with mean temperatures above the threshold should gain soil C with warming. Below the temperature threshold, the positive effect of warming on enzyme kinetics exceeds the negative effect of warming on CUE, microbial biomass, and enzyme production. Above the threshold, an increment of warming has a greater relative impact on CUE (which declines linearly toward zero with increasing temperature) than on enzyme kinetics.

Our analysis shows that temperature thresholds depend on CUE scenario and model complexity. For the microbial models, the greater the temperature sensitivity of CUE, the lower the temperature threshold for minimum SOC (Fig. 3). Under varied CUE, the temperature thresholds fell well below the reference temperature, so warming increased SOC and/or DOC and decreased MBC, ENZC, and CO_2 efflux. Under constant CUE, temperature thresholds were not observed, so warming decreased SOC and DOC and generally increased MBC, ENZC, and CO_2 efflux. Which of these scenarios will prevail in the coming century is unclear; soil CUE usually decreases with warming (Manzoni et al. 2012), but the response can vary with ecosystem and substrate chemistry (Frey et al. 2013). It is also possible that microbial CUE will adapt or acclimate to warming temperatures (Allison et al. 2010).

We found that the two microbial models with more C pools (i.e. AWB and MEND) predicted different temperature thresholds than the simpler GER model for a given CUE scenario (Fig. 3). For instance, under varied CUE, the threshold temperatures were 0.90, 1.45, and 7.95°C for MEND, AWB, and GER, respectively. When the CUE sensitivity to temperature was

289 intermediate (i.e. acclimated CUE), the threshold temperature was closer among models but still
290 followed the ranking MEND < AWB < GER. We attribute these differences in threshold
291 temperature to differences in model complexity, given that temperature and CUE were equal
292 across the models. Complexity includes both the difference in model structure—i.e. more pools
293 (MBC and ENZC) in AWB and MEND than GER—and the parameters associated with those
294 additional pools. Both factors likely contribute to the inter-model differences in threshold
295 temperature. However, the increased complexity of MEND relative to AWB led to a relatively
296 minor difference (<0.6 ºC) in the temperature threshold between these models. Thus subdivision
297 of major C pools into sub-components (i.e. MOC, POC, EM, and EP) had relatively little effect
298 on model predictions, at least under the CUE scenarios and parameters we examined.
299 *4.3 Differences in decomposition dynamics between models*
300 The three microbial models showed warming responses distinct from the conventional
301 model. This difference is mainly attributed to microbial control over decomposition through
302 enzyme-mediated processes (Schimel and Weintraub 2003) which are absent from first-order
303 decay models (Parton et al. 1987). Including microbial-enzyme processes couples the dynamics
304 of SOC and MBC pools, which has two main consequences in our analysis. First, reductions in
305 microbial biomass that occur due to warming effects on CUE tend to increase SOC pool sizes.
306 Thus the microbial models lose SOC under constant CUE and gain SOC under varied CUE
307 whereas CON always loses SOC with warming. Second, the coupling of the soil C and MBC
308 pools results in damped oscillations reminiscent of predator-prey dynamics. The amplitude and
309 period of oscillation depend on model parameters, specifically CUE, Vmax, and Km (Wang et al.
310 2013b). Though some first-order systems could also show damped oscillations (Bolker et al.

311 1998), CON did not, suggesting that its pools are not sufficiently coupled to produce oscillatory
312 responses to temperature change under these parameters.
313 Among the microbial models, oscillations were generally weaker in MEND and in the
314 acclimated CUE scenario. Greater complexity in MEND's structure likely contributed to
315 weakened oscillations, especially in relation to MOC, the largest SOC pool in MEND. The
316 MOC pool receives inputs from POC decomposition and loses C through MOC decomposition
317 (Eq. A45), whereas the SOC pools in the other microbial models receive constant external
318 inputs. The structure of MEND means that changes in microbial biomass and associated enzyme
319 production have counterbalancing effects on MOC inputs and losses, thereby weakening MOC
320 oscillations. For example, warming under varied CUE reduced MOC decomposition by EM but
321 also reduced MOC inputs from POC decomposition by EP (Fig. S2). Weaker oscillations
322 occurred under acclimated CUE in all microbial models because initial pool sizes were closer to
323 equilibrium pool sizes in this scenario. There was almost no net change in SOC with warming
324 because the temperature threshold for minimum SOC was near 20ºC for all three models under
325 acclimated CUE (Fig. 3).
326 Although the microbial models tended to show similar behaviors, we did find contrasting
327 DOC dynamics between AWB and MEND during the transient phase. In both models, DOC
328 pools are primarily controlled by inputs from SOC decomposition, but MEND has multiple SOC
329 pools that contribute to DOC flux. In AWB, increased decomposition of a single SOC pool
330 results in greater DOC production pool under constant CUE, whereas reduced SOC
331 decomposition reduces DOC under varied CUE. In MEND, the dynamics are more complex
332 because DOC dynamics are also influenced by decomposition of the POC pool. Under constant
333 CUE in MEND, the POC pool decomposes rapidly at first and supplies increased DOC. After a

few years, POC decomposition slows and POC pool size starts to recover, leading to lower DOC production and oscillations in DOC pools. Similar controls act in the varied and acclimated CUE scenarios, but the POC pool increases or changes little initially (due to reduced MBC), resulting in reduced DOC production. In MEND, the QOC pool equilibrates with DOC through sorption-desorption, and therefore the two pools show very similar dynamics.

4.5 Implications for global soil C projections

Our analyses show that both conventional and microbial models predict soil C losses in the decade immediately following warming. Thus all of these models are consistent with short-term observations from field and laboratory warming experiments (McGuire et al. 1995, Rustad et al. 2001, Melillo et al. 2002, Hartley et al. 2007, Bradford et al. 2008, Hartley et al. 2008, Melillo et al. 2011). However, our conventional model could not replicate the relatively rapid attenuation of soil respiration that is often observed following the initial increase (Luo et al. 2001, Knorr et al. 2005, Hartley et al. 2007, Bradford et al. 2008, Hartley et al. 2008, Zhou et al. 2012, Tucker et al. 2013). Ultimately, depletion of SOC and DOC substrates reduces CO_2 efflux to pre-warming levels even in CON, but this attenuation requires nearly 5 decades. In contrast, attenuation has the potential to be much more rapid in the microbial models, albeit followed by damped oscillations (Fig. 4). Other studies also show that microbial mechanisms are required to explain soil respiration responses. For example, including enzyme and microbial controls on decomposition improved the ability to simulate rewetting dynamics (Lawrence et al. 2009).

Our analysis reveals model properties that are relevant for scaling up microbial processes to the globe. In the microbial models, equilibrium SOC responses to warming depend on the initial soil temperature (Fig. 3). At initial temperatures below 8ºC in GER or 1ºC in AWB and MEND, SOC declines in response to warming under the varied CUE scenario, and the

357 temperature threshold increases as the temperature sensitivity of CUE declines. Thus the models
358 would predict SOC losses with warming in cold biomes, such as arctic tundra (Fig. 3). The
359 losses increase with lower temperature sensitivity of CUE. Warmer regions such as the tropics
360 could experience minimal SOC losses or even gains with warming, especially if CUE is highly
361 sensitive to temperature. This finding is consistent with observations that the temperature
362 sensitivity of SOC decomposition is regulated by native soil temperature (Ågren and Bosatta
363 2002).

364 Another key feature of the microbial models is a decoupling between equilibrium SOC
365 and inputs. Whereas SOC pool sizes are directly proportional to inputs in conventional models,
366 inputs have different effects on equilibrium SOC in the microbial models (Wang et al. 2013b) In
367 GER, equilibrium SOC has no mathematical dependence on inputs (Eq. A17), and in AWB and
368 MEND, equilibrium SOC depends on the ratio of SOC to DOC inputs but not the total amount
369 (Eqs. A29 and 52-53). This result explains why Allison et al. (2010) did not observe significant
370 changes in soil C when SOC and DOC inputs were both either increased or decreased. Likewise,
371 Wieder et al. (2013) observed little change in predicted global soil C following a simulated 20%
372 increase in global litter inputs. In these microbial models, MBC is directly proportional to inputs
373 such that increased inputs stimulate microbial growth and SOC turnover. This prediction, while
374 at odds with conventional models, is consistent with an analysis showing that NPP explains
375 under 10% of the global spatial variation in SOC stocks (Todd-Brown et al. 2013). However,
376 additional empirical analyses are needed to confirm whether spatial variation in SOC stocks is
377 better explained by microbial parameters.

378

379 **5. Conclusion**

Recent papers have called for integration of microbial-scale models into broad-scale land models (Todd-Brown et al. 2012, Treseder et al. 2012). Such efforts could help resolve the uncertainty in predictions from these broad-scale models (Todd-Brown et al. 2013, Wieder et al. 2013). Our model comparison indicates that both model complexity and the extent of CUE acclimation regulate decomposition dynamics with warming over decadal to centennial time scales. Furthermore, different model structures and parameterization resulted in different predictions for C pool responses to warming. Temperature thresholds that affect the magnitude and direction of SOC response to warming appear to be a common feature of microbial models. In addition, the most complex microbial model predicted less pronounced oscillations in soil C pools and fluxes. Together, these findings suggest that relatively simple microbial models could represent long-term SOC responses to climate, especially given the rapidly increasing availability of observations at short-term to long-term time scales.

Although the microbial models we analyzed made largely similar predictions at equilibrium, more complex models could improve the mechanistic representation of SOC dynamics on decadal time scales. Continuous change in climate over time may prevent soils from reaching equilibrium and require models that accurately predict transient dynamics. Whether these dynamics will take the form of strong oscillations is unclear, since global warming will occur gradually over decades to centuries, rather than as a step change in temperature. In addition, we cannot rule out the need for more complex models to describe short term processes in soil C dynamics (Zelenev et al. 2005) or other mechanisms that were not explored here, such as physiochemical changes, priming, and nitrogen interactions (Thornley and Cannell 2001, Fontaine et al. 2003, Thornton et al. 2009, Kuzyakov 2010, Li et al. 2013). Still,

our approach should be useful for optimizing microbial model complexity before integration into larger-scale models.

Acknowledgements

We thank two anonymous reviewers for their valuable and insightful comments. This research was funded by US National Science Foundation (NSF) grants DBI 0850290, EPS 0919466, DEB 0743778, DEB 0840964, EF 1137293, and EF 0928388 and was also funded in part by the Laboratory Directed Research and Development (LDRD) Program of the Oak Ridge National Laboratory (ORNL) and by the U.S. Department of Energy Biological and Environmental Research program. ORNL is managed by UT-Battelle, LLC, for the U.S. Department of Energy under contract DE-AC05-00OR22725. Part of the model runs were performed at the Supercomputing Center for Education & Research (OSCER), University of Oklahoma.

Appendix A

Conventional model (CON)

The conventional model is representative of first-order models of soil organic carbon (SOC) dynamics. This model includes SOC, dissolved organic C (DOC), and microbial biomass C (MBC) pools with the decomposition rate of each pool represented as a first-order process. The decay constant k_i increases exponentially with temperature according to the Arrhenius relationship:

$$k_i(T) = k_{i,ref} * \exp\left[-\frac{Ea_i}{R} * \left(\frac{1}{T} - \frac{1}{T_{ref}}\right)\right] \quad \text{(A1)}$$

where $k_{i,ref}$ is the decay constant at the reference temperature T_{ref} (Kelvin), and Ea_i is the activation energy with $i = D$, S, or C representing DOC, SOC, and MBC pools, respectively. R is the ideal gas constant, 8.314 J mol^{-1} K^{-1}. Decomposition of each pool is represented as:

$$F_S = k_S * S \quad \text{(A2)}$$

$$F_D = k_D * D \quad \text{(A3)}$$

$$F_B = k_B * B \quad \text{(A4)}$$

The change in the SOC pool is proportional to external inputs (I_S), transfers from the other pools, and losses due to first-order decomposition:

$$\frac{dS}{dt} = I_S + a_{DS} * F_D + a_B * a_{BS} * F_B - F_S \quad \text{(A5)}$$

where a_{DS} is the transfer coefficient from the DOC to the SOC pool, a_B is the transfer coefficient from the MBC to the DOC and SOC pools, and a_{BS} is the partition coefficient for dead microbial biomass between the SOC and DOC pools. Transfer coefficients can range from 0.0 to 1.0, with lower values indicating a larger fraction of C respired as CO_2. The change in the DOC pool is represented similarly, but includes a transfer from SOC to DOC in proportion to a_{SD} and a loss due to microbial uptake, $u * D$:

$$\frac{dD}{dt} = I_D + a_{SD} * F_S + a_B * (1 - a_{BS}) * F_B - u * D - F_D \quad \text{(A6)}$$

The change in the microbial biomass pool is the difference between uptake and turnover, where u represents the fraction h^{-1} of the DOC pool taken up by microbial biomass:

$$\frac{dB}{dt} = u * D - F_B \quad \text{(A7)}$$

The CO_2 respiration rate is the sum of the proportion of fluxes that do not enter soil pools:

$$C_R = F_S * (1 - a_{SD}) + F_D * (1 - a_{DS}) + F_B * (1 - a_B) \quad \text{(A8)}$$

Steady state analytical solution

The steady-state analytical solutions for the DOC, SOC, and MBC pools in CON are:

$$D = \frac{I_D + I_S * a_{SD}}{u + k_D + u * a_B * (a_{BS} - 1 - a_{BS} * a_{SD}) - a_{DS} * k_D * a_{SD}} \quad \text{(A9)}$$

$$S = \frac{I_S + D * (a_{DS} * k_D + u * a_B * a_{BS})}{k_S} \quad \text{(A10)}$$

$$B = \frac{u * D}{k_B} \quad \text{(A11)}$$

GER

The GER microbial model represents SOC change as a function of input rate I_S, microbial turnover r_B, MBC, and extracellular enzyme V_{max} and K_m:

$$\frac{dS}{dt} = I_S + r_B \cdot B - B \cdot \frac{V \cdot S}{K + S} \quad \text{(A12)}$$

C inputs and dead biomass enter the SOC pool, and SOC is lost through decomposition, which is assumed to be a Michaelis-Menten process represented by the last term in Eq. A12. MBC change is a function of microbial turnover and assimilation of decomposed soil organic C, which occurs with C use efficiency E_C:

$$\frac{dB}{dt} = E_C \cdot B \cdot \frac{V \cdot S}{K + S} - \tau_B \cdot B \quad \text{(A13)}$$

where E_C is a linear function of temperature with slope m:

$$E_C(T) = E_{C,ref} + m * (T - T_{ref}) \quad \text{(A14)}$$

The CO_2 respiration rate (C_R) is then the fraction of decomposition not assimilated by microbial biomass:

$$C_R = (1 - E_C) \cdot B \cdot \frac{V \cdot S}{K + S} \quad \text{(A15)}$$

V_{max} and K_m have an Arrhenius dependence on temperature, similar to Eq. A1 in the conventional model:

$$Y(T) = Y_{ref} * \exp\left[-\frac{Ea_Y}{R} * \left(\frac{1}{T} - \frac{1}{T_{ref}}\right)\right] \quad \text{(A16)}$$

Steady state analytical solution

The steady-state analytical solutions for the SOC and MBC pools in GER are:

$$S = \frac{r_B \cdot K}{E_C \cdot V - r_B}; \quad \frac{r_B}{V} < E_C < 1 \quad \text{(A17)}$$

$$B = \frac{I_S \cdot E_C}{r_B \cdot (1 - E_C)} \quad \text{(A18)}$$

where E_C must be larger than r_B/V, otherwise microbes cannot assimilate enough C to compensate for microbial turnover; if $E_C = 1$, then microbes respire no C, all C is assimilated, and biomass grows indefinitely.

AWB

AWB is a more complex version of GER that includes explicit DOC and ENZC pools. Microbial biomass increases with DOC uptake (F_U) times C use efficiency and declines with death (F_B) and enzyme production (F_E):

$$\frac{dB}{dt} = F_U * E_C - F_B - F_E \quad \text{(A19)}$$

where assimilation is a Michaelis-Menten function scaled to the size of the microbial biomass pool:

$$F_U = \frac{V_U * B * D}{K_U + D} \quad \text{(A20)}$$

Microbial biomass death is modeled as a first-order process with a rate constant r_B:

$$F_B = r_B * B \quad \text{(A21)}$$

Enzyme production is modeled as a constant fraction (r_E) of microbial biomass:

$$F_E = r_E * B \quad \text{(A22)}$$

Temperature sensitivities for V, V_U, K, and K_U follow the Arrhenius relationship as in Eq. A1. Note that this relationship differs from the published version of AWB that used a linear relationship for K and K_U temperature sensitivity. We used the Arrhenius relationship here to

facilitate comparison with the other models and used the parameter values from the linear relationship at 20ºC as the reference values in Eq. A1. CO_2 respiration is the fraction of DOC that is not assimilated into MBC:

$$C_R = F_U * (1 - E_C) \quad \text{(A23)}$$

The enzyme pool increases with enzyme production and decreases with enzyme turnover:

$$\frac{dE}{dt} = F_E - F_L \quad \text{(A24)}$$

where enzyme turnover is modeled as a first-order process with a rate constant r_L:

$$F_L = r_L * E \quad \text{(A25)}$$

The SOC pool increases with external inputs and a fraction of dead microbial biomass (a_{BS}) and decreases due to decomposition losses:

$$\frac{dS}{dt} = I_S + F_B * a_{BS} - F_S \quad \text{(A26)}$$

where decomposition of SOC is catalyzed according to Michaelis-Menten kinetics by the enzyme pool:

$$F_S = \frac{V * E * S}{K + S} \quad \text{(A27)}$$

The DOC pool receives external inputs, the remaining fraction of dead microbial biomass, the decomposition flux, and dead enzymes, while assimilation of DOC by microbial biomass is subtracted:

$$\frac{dD}{dt} = I_D + F_B * (1 - a_{BS}) + F_S + F_L - F_U \quad \text{(A28)}$$

Steady state analytical solution

The steady-state analytical solutions for SOC, DOC, MBC, and ENZC in AWB are:

$$S = \frac{-r_L * K * \left(I_S * \left(r_B * \left(1 + E_C * (a_{BS} - 1)\right) + r_E * (1 - E_C)\right) + E_C * I_D * a_{BS} * r_B\right)}{I_S * \left(r_B * \left(r_L * \left(1 + E_C * (a_{BS} - 1)\right)\right) + r_E * (r_L * (1 - E_C) - E_C * V)\right) + E_C * I_D * (a_{BS} * r_B * r_L - r_E * V)} \quad \text{(A29)}$$

which simplifies to the following if $I_D = I_S$:

$$S = \frac{-r_L * K * (r_B + r_E) * (1 - E_C) + 2 * E_C * a_{BS} * r_B}{r_L * (r_B + r_E) * (1 - E_C) + 2 * E_C * (a_{BS} * r_B * r_L - r_E * V)} \quad \text{(A30)}$$

$$D = \frac{K_U * (r_B + r_E)}{r_B + r_E - E_C * V_U} \quad \text{(A31)}$$

$$B = \frac{E_C * (I_D + I_S)}{(1 - E_C) * (r_B + r_E)} \quad \text{(A32)}$$

$$E = \frac{B * r_E}{r_L} \quad \text{(A33)}$$

MEND

Five C pools are considered in MEND: (i) particulate organic carbon (POC, represented by the variable *P* in model equations), (ii) mineral-associated organic carbon (MOC, *M*), (iii) active layer of MOC (*Q*) interacting with dissolved organic carbon through adsorption and desorption, (iv) dissolved organic carbon (DOC, *D*), (v) microbial biomass carbon (MBC, *B*), and (vi) extracellular enzymes (*EP* and *EM*). The component fluxes are DOC uptake by microbes (denoted by the flux F_1), POC decomposition (F_2), MOC decomposition (F_3), microbial growth respiration (F_4) and maintenance respiration (F_5), adsorption (F_6) and desorption (F_7), microbial mortality (F_8), enzyme production (F_9), and enzyme turnover (F_{10}). Model equations for each component are listed as follows:

$$F_1 = \frac{(V_D + m_R) * B * D}{E_C * (K_D + D)} \quad \text{(A34)}$$

$$F_2 = \frac{V_P * E_P * P}{K_P + P} \quad \text{(A35)}$$

$$F_3 = \frac{V_M * E_M * M}{K_M + M} \quad \text{(A36)}$$

$$F_4 = \left(\frac{1}{E_C} - 1\right) * \frac{V_D * B * D}{K_D + D} \quad \text{(A37)}$$

$$F_5 = \left(\frac{1}{E_C} - 1\right) * \frac{m_R * B * D}{K_D + D} \quad \text{(A38)}$$

$$F_6 = K_{ads} * D * \left(1 - \frac{Q}{Q_{max}}\right) \quad \text{(A39)}$$

$$F_7 = \frac{K_{des} * Q}{Q_{max}} \quad \text{(A40)}$$

$$F_8 = m_R * B * (1 - p_{EP} - p_{EM}) \quad \text{(A41)}$$

$$F_{9,EP} = p_{EP} * m_R * B;\ F_{9,EM} = p_{EM} * m_R * B \quad \text{(A42)}$$

$$F_{10,EP} = r_{EP} * E_P;\ F_{10,EM} = r_{EM} * E_M \quad \text{(A43)}$$

where V_i and K_i represent the V_{max} and K_m for enzymatic degradation of pool i, m_R is the maintenance respiration rate, Q_{max} is the maximum DOC sorption capacity, K_{des} and K_{ads} are the specific adsorption and desorption rates, p_i is the fraction of m_R associated with production of enzyme i, and r_i is the turnover rate of enzyme pool i. V_i, K_i, m_R, K_{des}, and K_{ads} follow Arrhenius temperature sensitivity similar to Eq. A1, and E_C is linearly dependent on temperature as in Eq. A14. The differential equations are as follows for the pools:

$$\frac{dP}{dt} = I_P + (1 - g_D) * F_8 - F_2 \quad \text{(A44)}$$

$$\frac{dM}{dt} = (1 - f_D) * F_2 - F_3 \quad \text{(A45)}$$

$$\frac{dQ}{dt} = F_6 - F_7 \quad \text{(A46)}$$

$$\frac{dB}{dt} = F_1 - (F_4 + F_5) - F_8 - (F_{9,EP} + F_{9,EM}) \quad \text{(A47)}$$

$$\frac{dD}{dt} = I_D + f_D * F_2 + g_D * F_8 + F_3 + (F_{10,EP} + F_{10,EM}) - F_1 - (F_6 + F_7) \quad \text{(A48)}$$

$$\frac{dE_P}{dt} = F_{9,EP} - F_{10,EP} \quad \text{(A49)}$$

$$\frac{dE_M}{dt} = F_{9,EM} - F_{10,EM} \quad \text{(A50)}$$

and the CO_2 respiration rate is calculated as:

$$C_R = F_4 + F_5 \tag{A51}$$

MEND represents microbial respiration as a fraction of assimilation (Eqs. A37 and A38) whereas GER and AWB represent respiration as a fraction of microbial uptake (Eqs. A15 and A23); note that these representations are algebraically identical with respect to CUE.

Steady state analytical solution

The steady state analytical solutions to the MEND differential equations are as follows:

$$P = \frac{K_P}{V_P * p_{EP} * E_C * \frac{(I_D/I_P)+1}{r_{EP} * A} - 1} \tag{A52}$$

$$M = \frac{K_M}{V_M * p_{EM} * \frac{E_C}{r_{EM} * (1-f_D) * A} * \left(1 + \frac{I_D}{I_P}\right) - 1} \tag{A53}$$

where

$$A = 1 - E_C + (1 - p_{EP} - p_{EM}) * E_C * (1 - g_D) * \left(\frac{I_D}{I_P} + 1\right) \tag{A54}$$

Eqs. A52-A53 simplify to the following if $I_D << I_P$:

$$P = \frac{K_P}{V_P * p_{EP} * \frac{E_C}{r_{EP} * (1 - g_D * E_C)} - 1} \tag{A55}$$

$$M = \frac{K_M}{V_M * p_{EM} * \frac{E_C}{r_{EM} * (1 - g_D * E_C) * (1 - f_D)} - 1} \tag{A56}$$

$$D = \frac{m_R * K_D}{V_D} \tag{A57}$$

$$Q = \frac{Q_{max}}{1 + \left(\frac{1}{D} * K_{BA}\right)} \tag{A58}$$

$$E_P = \frac{(B * m_R * p_{EP})}{r_{EP}} \tag{A59}$$

$$E_M = \frac{(B * m_R * p_{EM})}{r_{EM}} \quad \text{(A60)}$$

$$B = \frac{I_D + I_p}{\left(\frac{1}{E_C} - 1\right) * m_R} \quad \text{(A61)}$$

513
514

Table A1. Parameters used in model comparison.

Model	Parameter	Description	Value	Units
All	T_{ref}	Reference temperature	20	ºC
	$E_{C,ref}$	CUE at reference temperature	0.31	mg C mg^{-1} C
	m	CUE change with temperature	[0,-0.016]	ºC^{-1}
CON	I_S	SOC input rate	0.00015	mg C g^{-1} soil h^{-1}
	I_D	DOC input rate	0.00001	mg C g^{-1} soil h^{-1}
	$k_{S,ref}$	SOC decay rate	5×10^{-6}	mg C mg^{-1} C h^{-1}
	$k_{D,ref}$	DOC decay rate	0.001	mg C mg^{-1} C h^{-1}
	$k_{B,ref}$	MBC turnover rate	0.00028	mg C mg^{-1} C h^{-1}
	Ea_S	SOC activation energy	47	kJ mol^{-1} K^{-1}
	Ea_D	DOC activation energy	47	kJ mol^{-1} K^{-1}
	Ea_B	MBC activation energy	20	kJ mol^{-1} K^{-1}
	a_{DS}	DOC to SOC transfer coefficient	$E_C(T)$	
	a_{SD}	SOC to DOC transfer coefficient	$E_C(T)$	
	a_B	MBC to soil C transfer coefficient	$E_C(T)$	
	a_{BS}	Fraction of dead MBC transferred to SOC	0.5	
	u	DOC uptake rate	0.0005	mg C g^{-1} DOC h^{-1}
GER	I_S	SOC input rate	0.00016	mg C g^{-1} soil h^{-1}
	V_{ref}	SOC reference V_{max}	0.01	mg C mg^{-1} MBC h^{-1}
	K_{ref}	SOC reference K_m	250	mg C g^{-1} soil
	Ea_V	SOC V_{max} activation energy	47	kJ mol^{-1} K^{-1}
	Ea_K	SOC K_m activation energy	30	kJ mol^{-1} K^{-1}

	r_B	MBC turnover rate (same as $k_{B,ref}$ in CON)	0.00028	mg C mg^{-1} C h^{-1}
AWB	I_S	SOC input rate	0.00015	mg C g^{-1} soil h^{-1}
	I_D	DOC input rate	0.00001	mg C g^{-1} soil h^{-1}
	V_{ref}	SOC reference V_{max}	1	mg C mg^{-1} C h^{-1}
	$V_{U,ref}$	DOC uptake reference V_{max} (similar to V_{ref} in GER)	0.01	mg C mg^{-1} MBC h^{-1}
	K_{ref}	SOC reference K_m	250	mg C g^{-1} soil
	$K_{U,ref}$	DOC uptake reference K_m	0.26	mg C g^{-1} soil
	Ea_V	SOC V_{max} activation energy	47	kJ mol^{-1} K^{-1}
	Ea_{VU}	Uptake V_{max} activation energy	47	kJ mol^{-1} K^{-1}
	Ea_K	SOC K_m activation energy	30	kJ mol^{-1} K^{-1}
	Ea_{KU}	Uptake K_m activation energy	30	kJ mol^{-1} K^{-1}
	r_B	MBC turnover rate (same as $k_{B,ref}$ in CON)	0.00028	mg C mg^{-1} C h^{-1}
	r_E	Enzyme production rate (same as r_{EP}+r_{EM} in MEND)	5.6×10^{-6}	mg C mg^{-1} MBC h^{-1}
	r_L	Enzyme loss rate	0.001	mg C mg^{-1} C h^{-1}
	a_{BS}	Fraction of dead MBC transferred to SOC	0.5	
MEND	I_P	POC input rate	0.00015	mg C g^{-1} soil h^{-1}
	I_D	DOC input rate	0.00001	mg C g^{-1} soil h^{-1}
	$V_{D,ref}$	DOC reference V_{max} (same as u in CON)	0.0005	mg C mg^{-1} C h^{-1}
	$V_{P,ref}$	POC reference V_{max}	2.5	mg C mg^{-1} C h^{-1}
	$V_{M,ref}$	MOC reference V_{max}	1	mg C mg^{-1} C h^{-1}
	$K_{D,ref}$	DOC reference K_m (same as $K_{U,ref}$ in AWB)	0.26	mg C g^{-1} soil
	$K_{P,ref}$	POC reference K_m	50	mg C g^{-1} soil

	$K_{M,ref}$	MOC reference K_m	250	mg C g^{-1} soil
	$K_{ads,ref}$	Reference specific adsorption rate	0.006	mg C mg^{-1} C h^{-1}
	$K_{des,ref}$	Reference specific desorption rate	0.001	mg C mg^{-1} C h^{-1}
	$m_{R,ref}$	Reference specific maintenance factor (same as r_B in AWB)	0.00028	mg C mg^{-1} C h^{-1}
	Ea_{VD}	DOC V_{max} activation energy	47	kJ mol^{-1} K^{-1}
	Ea_{VP}	POC V_{max} activation energy	45	kJ mol^{-1} K^{-1}
	Ea_{VM}	MOC V_{max} activation energy	47	kJ mol^{-1} K^{-1}
	Ea_{KD}	DOC K_m activation energy	30	kJ mol^{-1} K^{-1}
	Ea_{KP}	POC K_m activation energy	30	kJ mol^{-1} K^{-1}
	Ea_{KM}	MOC K_m activation energy	30	kJ mol^{-1} K^{-1}
	Ea_{Kads}	Adsorption activation energy	5	kJ mol^{-1} K^{-1}
	Ea_{Kdes}	Desorption activation energy	20	kJ mol^{-1} K^{-1}
	Ea_{mR}	Maintenance activation energy (analogous to Ea_B in CON)	20	kJ mol^{-1} K^{-1}
	Q_{max}	Maximum DOC sorption capacity	1.7	mg C g^{-1} soil
	p_{EP}	Fraction of m_R allocated to POC enzyme production	0.01	
	p_{EM}	Fraction of m_R allocated to MOC enzyme production	0.01	
	r_{EP}	POC enzyme loss rate	0.001	mg C mg^{-1} C h^{-1}
	r_{EM}	MOC enzyme loss rate	0.001	mg C mg^{-1} C h^{-1}
	g_D	Fraction of dead MBC transferred to SOC (same as a_{BS} in AWB)	0.5	
	f_D	Fraction of decomposed POC allocated to DOC	0.5	

References

Ågren, G. I. and E. Bosatta. 2002. Reconciling differences in predictions of temperature response of soil organic matter. Soil Biology and Biochemistry **34**:129-132.

Ågren, G. I. and J. Å. M. Wetterstedt. 2007. What determines the temperature response of soil organic matter decomposition? Soil Biology and Biochemistry **39**:1794-1798.

Allison, S. D., M. D. Wallenstein, and M. A. Bradford. 2010. Soil-carbon response to warming dependent on microbial physiology. Nature Geoscience **3**:336-340.

Bolker, B. M., S. W. Pacala, and W. J. Parton. 1998. LINEAR ANALYSIS OF SOIL DECOMPOSITION: INSIGHTS FROM THE CENTURY MODEL. Ecological Applications **8**:425-439.

Bradford, M. A., C. A. Davies, S. D. Frey, T. R. Maddox, J. M. Melillo, J. E. Mohan, J. F. Reynolds, K. K. Treseder, and M. D. Wallenstein. 2008. Thermal adaptation of soil microbial respiration to elevated temperature. Ecology Letters **11**:1316-1327.

del Giorgio, P. A. and J. J. Cole. 1998. Bacterial growth efficiency in natural aquatic systems. Annual Review of Ecology and Systematics **29**:503-541.

Devevre, O. C. and W. R. Horwath. 2000. Decomposition of rice straw and microbial carbon use efficiency under different soil temperatures and moistures. Soil Biology & Biochemistry **32**:1773-1785.

Fontaine, S., A. Mariotti, and L. Abbadie. 2003. The priming effect of organic matter: a question of microbial competition? Soil Biology & Biochemistry **35**:837-843.

Frey, S. D., J. Lee, J. M. Melillo, and J. Six. 2013. The temperature response of soil microbial efficiency and its feedback to climate. Nature Clim. Change **3**:395-398.

Friedlingstein, P., P. Cox, R. Betts, L. Bopp, W. Von Bloh, V. Brovkin, P. Cadule, S. Doney, M. Eby, I. Fung, G. Bala, J. John, C. Jones, F. Joos, T. Kato, M. Kawamiya, W. Knorr, K. Lindsay, H. D. Matthews, T. Raddatz, P. Rayner, C. Reick, E. Roeckner, K. G. Schnitzler, R. Schnur, K. Strassmann, A. J. Weaver, C. Yoshikawa, and N. Zeng. 2006. Climate-carbon cycle feedback analysis: Results from the (CMIP)-M-4 model intercomparison. Journal of Climate **19**:3337-3353.

German, D. P., K. R. B. Marcelo, M. M. Stone, and S. D. Allison. 2012. The Michaelis-Menten kinetics of soil extracellular enzymes in response to temperature: a cross-latitudinal study. Global Change Biology **18**:1468-1479.

Hartley, I. P., A. Heinemeyer, and P. Ineson. 2007. Effects of three years of soil warming and shading on the rate of soil respiration: substrate availability and not thermal acclimation mediates observed response. Global Change Biology **13**:1761-1770.

Hartley, I. P., D. W. Hopkins, M. H. Garnett, M. Sommerkorn, and P. A. Wookey. 2008. Soil microbial respiration in arctic soil does not acclimate to temperature. Ecology Letters **11**:1092-1100.

Jobbagy, E. G. and R. B. Jackson. 2000. The vertical distribution of soil organic carbon and its relation to climate and vegetation. Ecological Applications **10**:423-436.

Knorr, W., I. C. Prentice, J. I. House, and E. A. Holland. 2005. Long-term sensitivity of soil carbon turnover to warming. Nature **433**:298-301.

Kuzyakov, Y. 2010. Priming effects: Interactions between living and dead organic matter. Soil Biology & Biochemistry **42**:1363-1371.

Lawrence, C. R., J. C. Neff, and J. P. Schimel. 2009. Does adding microbial mechanisms of decomposition improve soil organic matter models? A comparison of four models using data from a pulsed rewetting experiment. Soil Biology & Biochemistry **41**:1923-1934.

Li, J., S. E. Ziegler, C. S. Lane, and S. A. Billings. 2013. Legacies of native climate regime govern responses of boreal soil microbes to litter stoichiometry and temperature. Soil Biology and Biochemistry **66**:204-213.

567 Luo, Y. Q., S. Q. Wan, D. F. Hui, and L. L. Wallace. 2001. Acclimatization of soil respiration to warming in a
568 tall grass prairie. Nature **413**:622-625.
569 Malcolm, G. M., J. C. Lopez-Gutierrez, R. T. Koide, and D. M. Eissenstat. 2008. Acclimation to
570 temperature and temperature sensitivity of metabolism by ectomycorrhizal fungi. Global
571 Change Biology **14**:1169-1180.
572 Manzoni, S. and A. Porporato. 2007. A theoretical analysis of nonlinearities and feedbacks in soil carbon
573 and nitrogen cycles. Soil Biology and Biochemistry **39**:1542-1556.
574 Manzoni, S., P. Taylor, A. Richter, A. Porporato, and G. I. Agren. 2012. Environmental and stoichiometric
575 controls on microbial carbon-use efficiency in soils. New Phytologist **196**:79-91.
576 McGuire, A. D., J. M. Melillo, D. W. Kicklighter, and L. A. Joyce. 1995. Equilibrium responses of soil
577 carbon to climate change: Empirical and process-based estimates. Journal of Biogeography
578 **22**:785-796.
579 Melillo, J. M., S. Butler, J. Johnson, J. Mohan, P. Steudler, H. Lux, E. Burrows, F. Bowles, R. Smith, L. Scott,
580 C. Vario, T. Hill, A. Burton, Y. M. Zhou, and J. Tang. 2011. Soil warming, carbon-nitrogen
581 interactions, and forest carbon budgets. Proceedings of the National Academy of Sciences of the
582 United States of America **108**:9508-9512.
583 Melillo, J. M., P. A. Steudler, J. D. Aber, K. Newkirk, H. Lux, F. P. Bowles, C. Catricala, A. Magill, T. Ahrens,
584 and S. Morrisseau. 2002. Soil warming and carbon-cycle feedbacks to the climate system.
585 Science **298**:2173-2176.
586 Parton, W. J., D. S. Schimel, C. V. Cole, and D. S. Ojima. 1987. Analysis of Factors Controlling Soil Organic-
587 Matter Levels in Great-Plains Grasslands. Soil Science Society of America Journal **51**:1173-1179.
588 Parton, W. J., J. W. B. Stewart, and C. V. Cole. 1988. Dynamics of C, N, P and S in Grassland Soils - a
589 Model. Biogeochemistry **5**:109-131.
590 Rustad, L. E., J. L. Campbell, G. M. Marion, R. J. Norby, M. J. Mitchell, A. E. Hartley, J. H. C. Cornelissen, J.
591 Gurevitch, and Gcte-News. 2001. A meta-analysis of the response of soil respiration, net
592 nitrogen mineralization, and aboveground plant growth to experimental ecosystem warming.
593 Oecologia **126**:543-562.
594 Schimel, J. 2013. Soil carbon: Microbes and global carbon. Nature Clim. Change **3**:867-868.
595 Schimel, J. P. and M. N. Weintraub. 2003. The implications of exoenzyme activity on microbial carbon
596 and nitrogen limitation in soil: a theoretical model. Soil Biology & Biochemistry **35**:549-563.
597 Sinsabaugh, R. L., R. K. Antibus, and A. E. Linkins. 1991. An Enzymatic Approach to the Analysis of
598 Microbial Activity during Plant Litter Decomposition. Agriculture Ecosystems & Environment
599 **34**:43-54.
600 Sinsabaugh, R. L., S. Manzoni, D. L. Moorhead, and A. Richter. 2013. Carbon use efficiency of microbial
601 communities: stoichiometry, methodology and modelling. Ecol Lett **16**:930-939.
602 Six, J., S. D. Frey, R. K. Thiet, and K. M. Batten. 2006. Bacterial and fungal contributions to carbon
603 sequestration in agroecosystems. Soil Science Society of America Journal **70**:555-569.
604 Thornley, J. H. M. and M. G. R. Cannell. 2001. Soil Carbon Storage Response to Temperature: an
605 Hypothesis. Annals of Botany **87**:591-598.
606 Thornton, P. E., S. C. Doney, K. Lindsay, J. K. Moore, N. Mahowald, J. T. Randerson, I. Fung, J. F.
607 Lamarque, J. J. Feddema, and Y. H. Lee. 2009. Carbon-nitrogen interactions regulate climate-
608 carbon cycle feedbacks: results from an atmosphere-ocean general circulation model.
609 Biogeosciences **6**:2099-2120.
610 Todd-Brown, K. E. O., F. M. Hopkins, S. N. Kivlin, J. M. Talbot, and S. D. Allison. 2012. A framework for
611 representing microbial decomposition in coupled climate models. Biogeochemistry **109**:19-33.
612 Todd-Brown, K. E. O., J. T. Randerson, W. M. Post, F. M. Hoffman, C. Tarnocai, E. A. G. Schuur, and S. D.
613 Allison. 2013. Causes of variation in soil carbon simulations from CMIP5 Earth system models
614 and comparison with observations. Biogeosciences **10**:1717-1736.

615 Treseder, K. K., T. C. Balser, M. A. Bradford, E. L. Brodie, E. A. Dubinsky, V. T. Eviner, K. S. Hofmockel, J. T.
616 Lennon, U. Y. Levine, B. J. MacGregor, J. Pett-Ridge, and M. P. Waldrop. 2012. Integrating
617 microbial ecology into ecosystem models: challenges and priorities. Biogeochemistry **109**:7-18.
618 Tucker, C. L., J. Bell, E. Pendall, and K. Ogle. 2013. Does declining carbon-use efficiency explain thermal
619 acclimation of soil respiration with warming? Global Change Biology **19**:252-263.
620 Wang, G. and W. M. Post. 2012. A theoretical reassessment of microbial maintenance and implications
621 for microbial ecology modeling. FEMS Microbiology Ecology **81**:610-617.
622 Wang, G. S., W. M. Post, and M. A. Mayes. 2013a. Development of microbial-enzyme-mediated
623 decomposition model parameters through steady-state and dynamic analyses. Ecological
624 Applications **23**:255-272.
625 Wang, Y. P., B. C. Chen, W. R. Wieder, Y. Q. Luo, M. Leite, B. E. Medlyn, M. Rasmussen, M. J. Smith, F. B.
626 Agusto, and F. Hoffman. 2013b. Oscillatory behavior of two nonlinear microbial models of soil
627 carbon decomposition. Biogeosciences Discuss. **10**:19661-19700.
628 Wieder, W. R., G. B. Bonan, and S. D. Allison. 2013. Global soil carbon projections are improved by
629 modelling microbial processes. Nature Clim. Change **3**:909-912.
630 Zelenev, V. V., A. H. C. van Bruggen, and A. M. Semenov. 2005. Short-Term Wavelike Dynamics of
631 Bacterial Populations in Response to Nutrient Input from Fresh Plant Residues. Microbial
632 Ecology **49**:83-93.
633 Zhou, J. Z., K. Xue, J. P. Xie, Y. Deng, L. Y. Wu, X. H. Cheng, S. F. Fei, S. P. Deng, Z. L. He, J. D. Van
634 Nostrand, and Y. Q. Luo. 2012. Microbial mediation of carbon-cycle feedbacks to climate
635 warming. Nature Climate Change **2**:106-110.

636

637

638

Table 1. Steady state C pool sizes (mg C g^{-1} soil) at the reference temperature (i.e. 20°C) for four models. CON denotes a conventional model described in Allison et al. (2010); GER, AWB, and MEND are three microbial models described in German et al. (2012), Allison et al. (2010), and Wang et al. (2013), respectively. SOC: soil organic carbon; POC: particulate organic carbon; MOC: mineral-associated organic carbon; DOC: dissolved organic carbon; QOC: mineral-associated DOC; MBC: microbial biomass carbon; ENZC: extracellular enzyme; EP: POC associated extracellular enzyme; EM: MOC associated enzyme.

Model	SOC	POC	MOC	DOC	QOC	MBC	ENZC	EP	EM
CON	33.36	-	-	0.04	-	0.08	-	-	-
GER	24.82	-	-	-	-	0.26	-	-	-
AWB	37.82	-	-	0.03	-	0.25	0.0014	-	-
MEND	43.51	5.75	36.97	0.15	0.79	0.26	0.0014	0.0007	0.0007

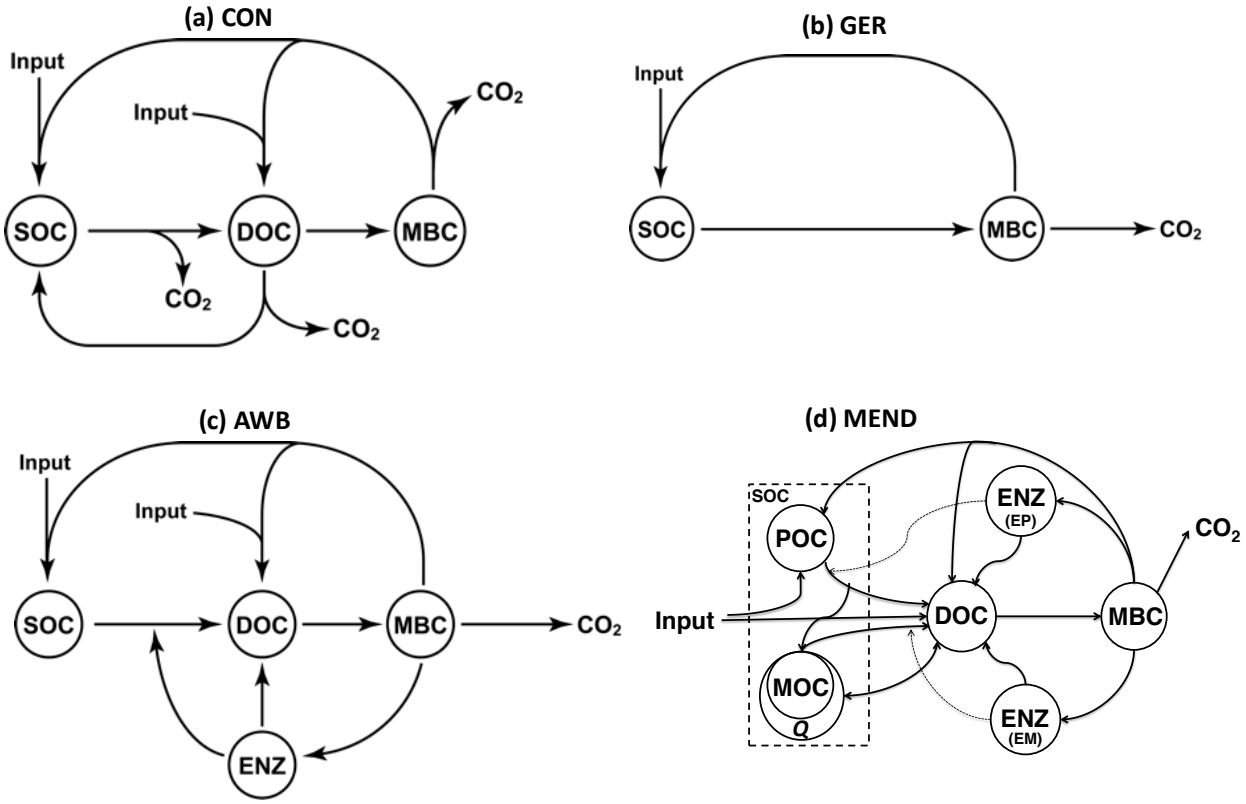

Figure 1. Model structures of (a) CON, (b) GER, (c) AWB and (d) MEND as modified from Allison et al. (2010) (CON, AWB), German et al. (2012) (GER) and Wang et al. (2013) (MEND). Abbreviations are given in Table 1.

658

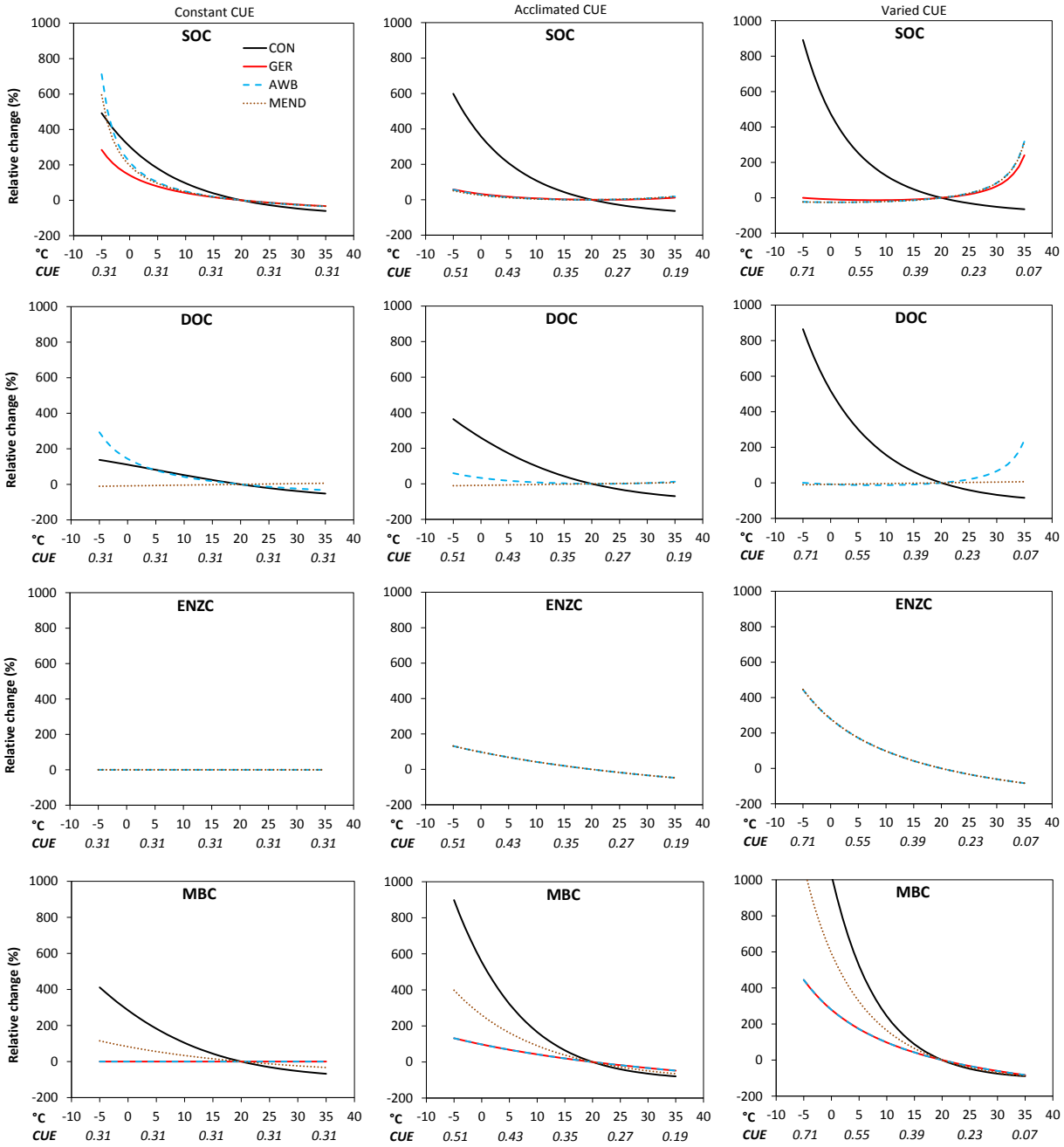
Constant CUE
Acclimated CUE
Varied CUE
SOC
DOC
ENZC
MBC
CON
GER
AWB
MEND
Relative change (%)
°C
CUE
0.31 0.31 0.31 0.31 0.31
0.51 0.43 0.35 0.27 0.19
0.71 0.55 0.39 0.23 0.07

659
660

Figure 2. Modeled relative changes (%) in steady state SOC, DOC, MBC, and ENZC as a function of temperature predicted by CON, GER, AWB, and MEND under constant, acclimated, and varied carbon use efficiency (CUE) scenarios. There are four models for SOC and MBC, three models for DOC, and two models for ENZC.

667

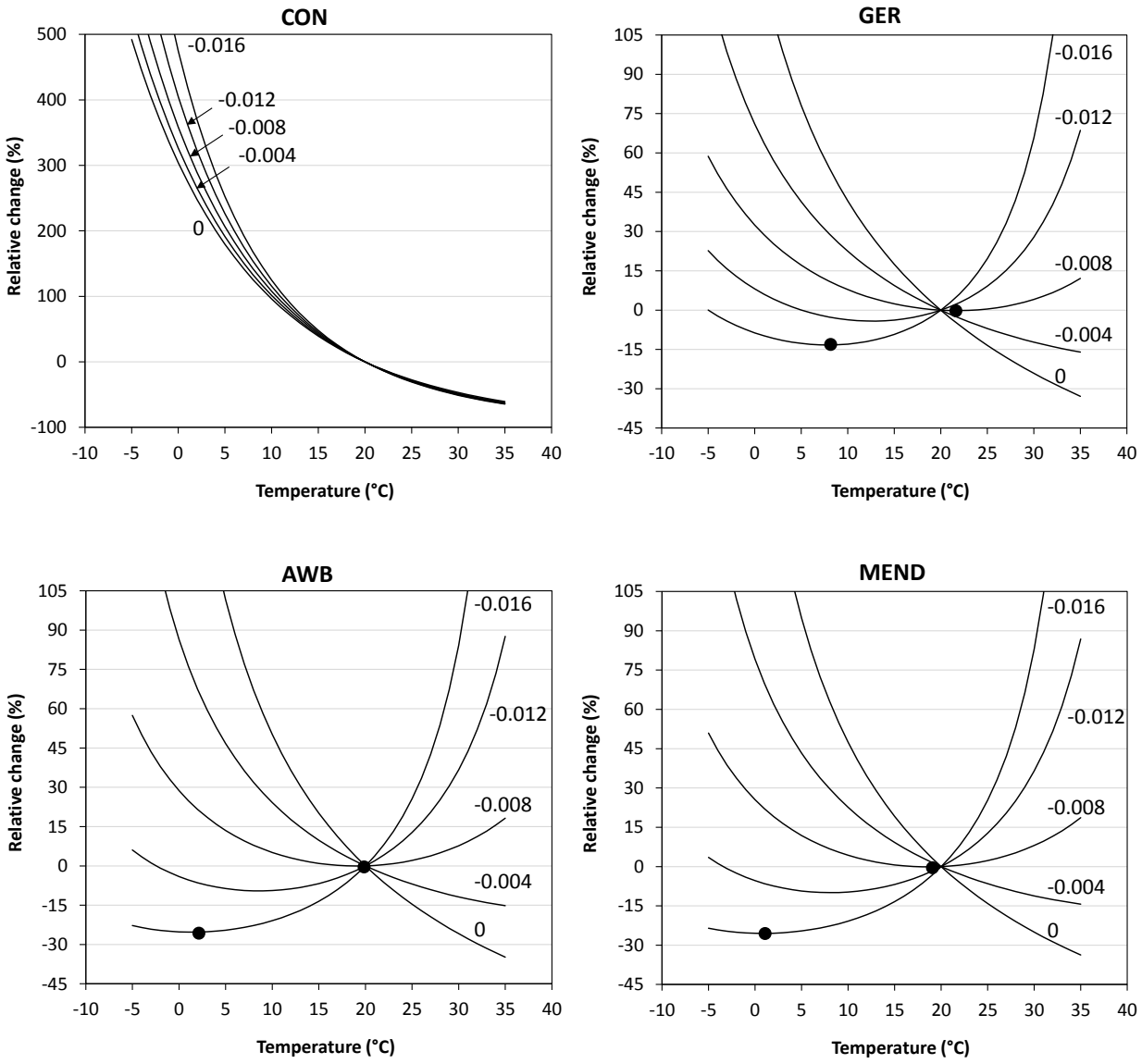

668

669 Figure 3: Modeled relative changes (%) in steady state SOC as a function of temperature (-5 to
670 35°C) predicted by CON, GER, AWB, and MEND under varying carbon use efficiency (CUE)
671 scenarios. Each line corresponds to a different CUE temperature response coefficient (*m*). Filled
672 circles denote the threshold temperatures associated with minimum SOC pool sizes under varied
673 (*m* = -0.016) and acclimated (*m* = -0.008) CUE scenarios, respectively. See Methods for details
674 on the model descriptions and CUE scenarios.

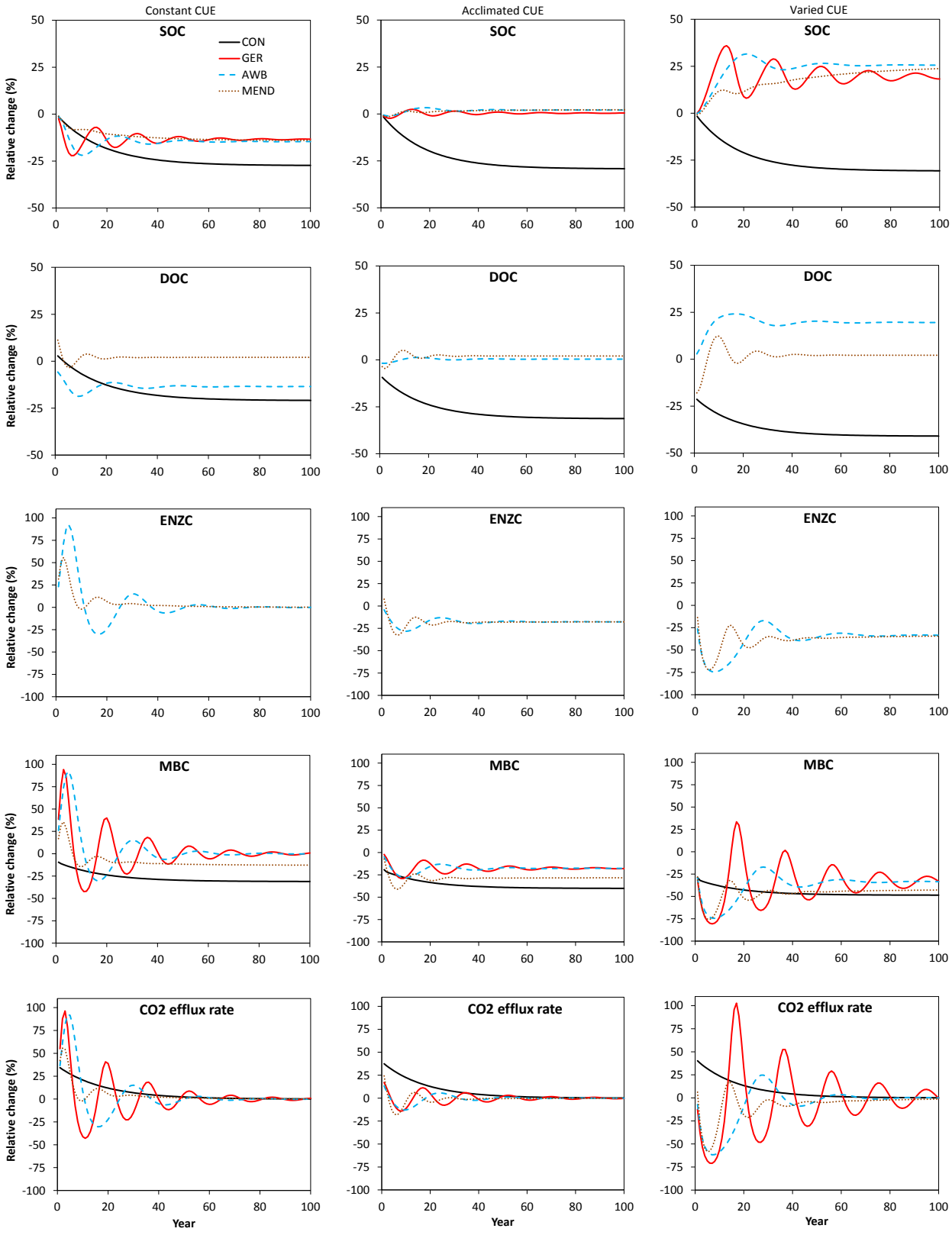
Constant CUE
Acclimated CUE
Varied CUE
SOC
DOC
ENZC
MBC
CO2 efflux rate
CON
GER
AWB
MEND
Relative change (%)
Year

675
676

677
678 Figure 4: Modeled relative changes (%) in SOC, DOC, MBC, ENZC, and CO_2 efflux with 5°C
679 warming under constant, acclimated, and varied CUE scenarios. See Methods for details on the
680 model descriptions and CUE scenarios.
681